Bull. Inst. Chem. Res., Kyoto Univ., Vol. 55, No. 1, 1977

Radical Chromatographic Separation and ESR Detection of Spin-trapped Nucleotide Radicals in Gamma-Irradiated Aqueous Solution

Hiroyuki HATANO, Souji ROKUSHIKA,** and Shiro KOMINAMI**

Received December 27, 1976

Aqueous solutions of nucleotides, uridine-5′-monophosphate, thymidine-5′-monophosphate and cytidine-5′-monophosphate, were irradiated with ^{60}Co γ-rays. Unstable intermediate radicals produced from the nucleotides were trapped by a spin-trapping reagent, 2-methyl-2-nitrosopropane, which was co-existing in the irradiated solutions, to produce relatively stable nitroxide radicals. Mixtures of the stable nitroxide radicals of the γ-irradiated nucleotides were separated on an ion exchange resin column and were detected by a flow esr method. The separated radicals were characterized by their esr spectra. Original unstable radicals were identified by the esr spectra of the derived nitroxide radicals. From the results of these radical chromatographic separation and esr detection of the spin-trapped nucleotide radicals, combining with other chemical measurements, radicals of N–1, N–3, C–5, and C–6 positions of the base moieties were found to produce in the γ-irradiated aqueous solutions of the nucleotides. This radical chromatographic method with esr detection is useful for determination of radiolytic radical products of organic or bio-molecules.

I. INTRODUCTION

Radical intermediates in γ-irradiated aqueous solutions of bio-molecules have been observed by esr methods during pulse radiolysis and during *in situ* radiolyses. Reaction mechanisms of the radiolyses have been presumed from the results about the esr observations of a rapid flow esr technique and of an esr simulation method. Pulse and *in situ* radiolyses, and rapid flow esr and esr simulation techniques, have made large contributions to the radiation chemistry of organic and bio-molecules in aqeous solutions. However, these methods involve expensive instruments and limited application.

Recently, the spin-trapping technique in esr studies has been developed by which short-lived radicals are derived to the more stable nitroxide radicals by reaction with the spin-trapping reagents such as nitroso or nitron compounds. Generally, the spin-trapping reactions are as follows:

$$R^1\cdot + R^2\text{–}N{=}O \longrightarrow R^1\text{–}\underset{\underset{O\cdot}{|}}{N}\text{–}R^2 \qquad (1)$$

$$R^1\cdot + R^2\text{–}CH{=}\underset{\underset{O}{\downarrow}}{N}\text{–}R^3 \longrightarrow R^1\text{–}\underset{\underset{R^2}{|}}{CH}\text{–}\underset{\underset{O\cdot}{|}}{N}\text{–}R^3 \qquad (2)$$

* 波多野博行，六鹿宗治：Department of Chemistry, Faculty of Science, Kyoto University, Kyoto.
** 小南思郎：Department of Environmental Sciences, Faculty of Integrated Art and Sciences, Hiroshima University, Hiroshima 730.

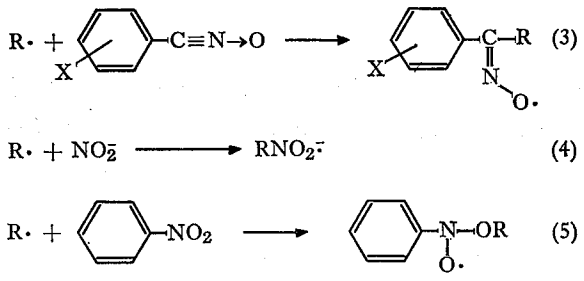

The structure of the short-lived radical can be characterized from the ser spectrum of the stable nitroxide radical in the irradiated solution. The unstable radical intermediates produced from several amino acids and nucleic acid constituents in γ-irradiated aqueous solution were investigated by the spin-trapping method by Taniguchi and Hatano.[1,2] This spin-trapping method is useful for the detection of the short-lived radicals produced in γ-irradiated solution. Most of the nitroxide radicals, however, show quite similar esr spectra from which it is very difficult to identify the structure of the radicals when the esr spectra of a mixture of more than one species are observed in the same solution.

High performance liquid chromatography has been recently combined with the spin-trapping method for separation and detection of radical species by Taniguchi, Rokushika, and Hatano.[3] This technique made it possible to separate the nitroxide radicals in the aqueous solutions of nucleotides, uridine-5′-monophosphate (5′-UMP), thymidine-5′-monophosphate (5′-TMP), and cytidine-5′-monophosphate (5′-CMP), during γ-irradiation when 2-methyl-2-nitrosopropane was used as a spin-trapping reagent in these studies.[4,5]

II. EXPERIMENTAL

Uridine-5′-monophosphate(5′-UMP), thymidine-5′-monophosphate (5′-TMP) and cytidine-5′-monophosphate (5′-CMP) were obtained from KOHJIN Co, Tokyo. 2-Methyl-2-nitrosopropane was synthesized according to the method of Stowell.[6] Anion exchange resin, Aminex A-27, was from Bio-Rad Laboratories, Richmond, California. All the other chemicals were purchased from Nakarai Chemicals Co., Kyoto.

Aerated aqueous solutions of 0.01 M 5′-UMP, 0.01 M 5′-TMP and 0.01 M 5′-CMP containing 0.025 M 2-methyl-2-nitrosopropane (t-BuNO) were irradiated at ice temperature with ^{60}Co γ-rays* at a dose rate of 6.6×10^4 rad/hr to a total dose of 1.3×10^5 rad. Immediately after the irradiation, about 70 ml of the irradiated solution was mixed with about 30 ml of 0.01 M phosphate buffer, pH 7.0, and loaded onto an Aminex A-27 column, 0.9 cm in dia. and 27 cm in length. A flow diagram of the chromatographic system was illustrated in Fig. 1, and an actual view of the radical chromatograph is illustrated in the Photo. An esr spectrometer, JEOL

* The facility of ^{60}Co-γ-ray irradiation of the Institute for Chemical Research, Kyoto University was used.

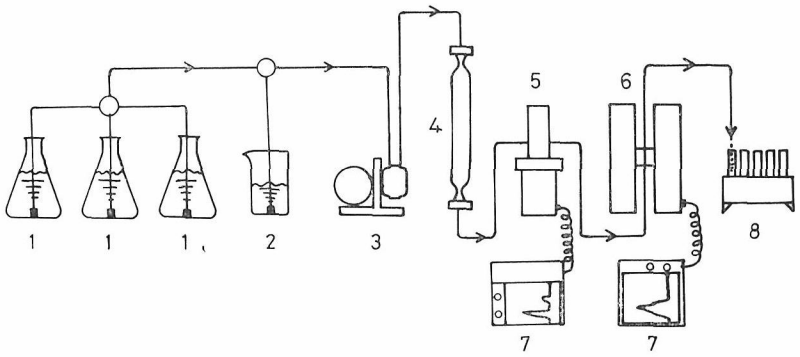

Fig. 1. A flow diagram of the radical chromatograph.
1: Reservoirs; 2: Sample; 3: Minipump; 4: Column; 5: UV Detector;
6: ESR Detector; 7: Recorders; 8: Fraction Collector.

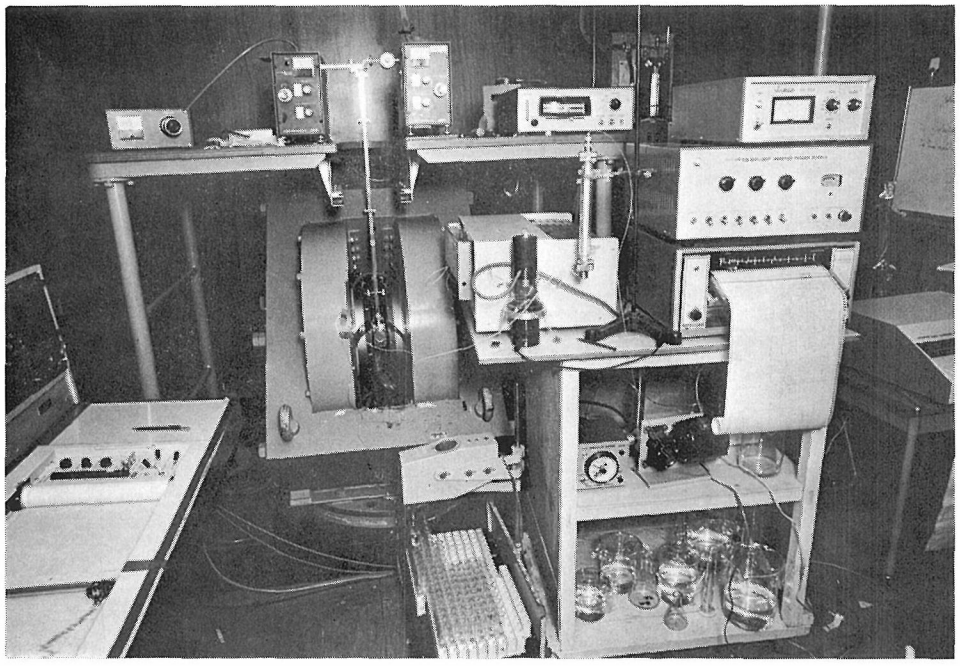

Photo: Radical Chromatograph (Hatano 1975)

PE-3X, which operated with X-band, was used as a radical detector in this experiments. An UV detector, a JASCO UV-254 photometer or a JASCO UVIDEC 100 spectrophotometer, was used simultaneously with the esr detector. Elutions were carried out sequentially for the chromatography, which are shown in Figs. 2, 3, and 4. Detection of esr spectra was performed by the flowing technique as described in the papers.[4,5] The eluate was passed through esr and UV detectors and collected by a fraction collector. The amount of residual sugar moieties at each fraction was determined by the orcinol method which revealed the sugar content as an absorbance at 675 nm and by the phenol-H_2SO_4 method which revealed the content as an absorbance at 490 nm. These were plotted in Figs. 2, 3, and 4.

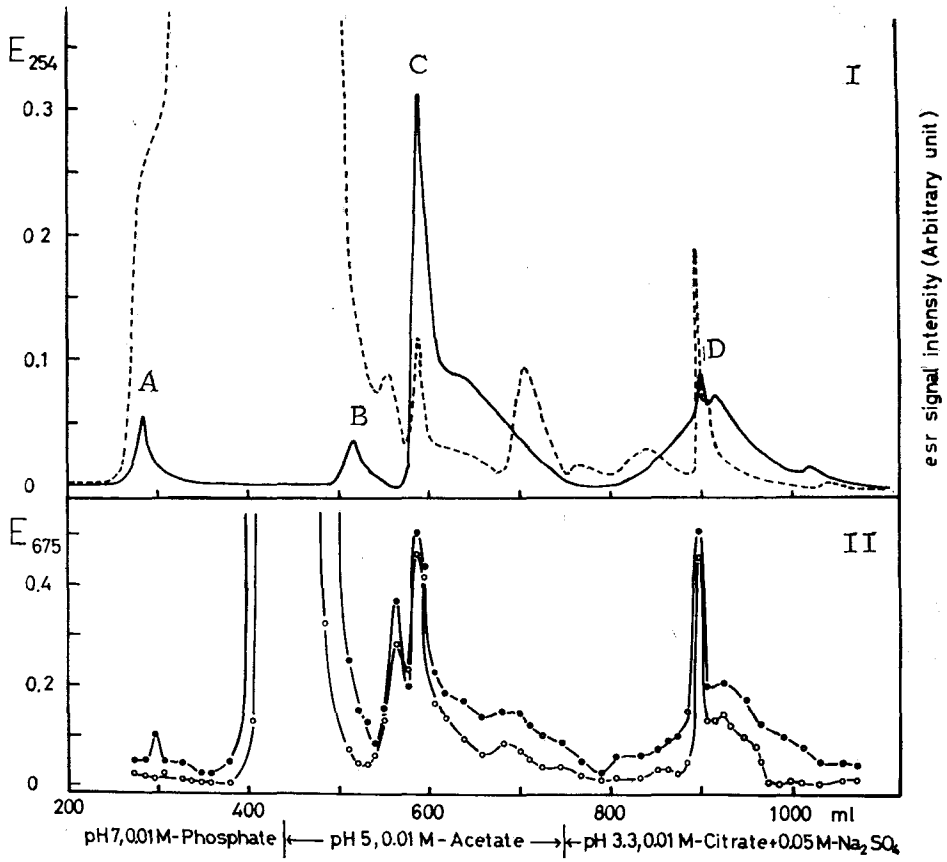

Fig. 2. Chromatogram of Spin Adducts of 5′-Uridine monophosphate and 2-Methyl-2-nitrosopropane.
Irradiation dose: 130 krads in aqueous solution with air at ice cold temperature; Chromatographic column: Aminex A-27, 0.9×23 cm at 22°C; Flow rate: 2.2 ml/min under 30 kg/cm^2 pressure; Detection: (I) ---- at 254 nm, —— esr, (II) —●— Orcinol-HCl reaction before reduction, —○— after reduction; Peaks A, B, C, and D: See text.

III. RESULTS

An air-saturated aqueous solution containing 0.01 M 5′-UMP and 0.025 M t-BuNO, that of 5′-TMP and that of 5′-CMP were cooled in an ice-bath and γ-irradiated to a total dose of 1.0×10^5 rad, which showed the esr spectra of Figs. 5, 6, and 7 respectively. Total amount of radicals increased linearly with dose to 1×10^5 rad, and the G-value was estimated to be 0.8 ± 0.2. The line shapes of the esr spectra of the irradiated solutions were independent of the dose in a range from 1×10^4 to 2×10^5 rad. Decay of esr signals was observed at room temperature which was about 10 % of the original after one hour, and no significant change in the line shapes was detected. The esr spectra in Figs. 5, 6, and 7 had a number of groups of complicated signals and it seemed to be impossible to analyse these spectra without separation of the radicals. Liquid chromatography was applied for the solutions immediately after irradiation which showed the chromatograms of Figs. 2, 3, and 4.

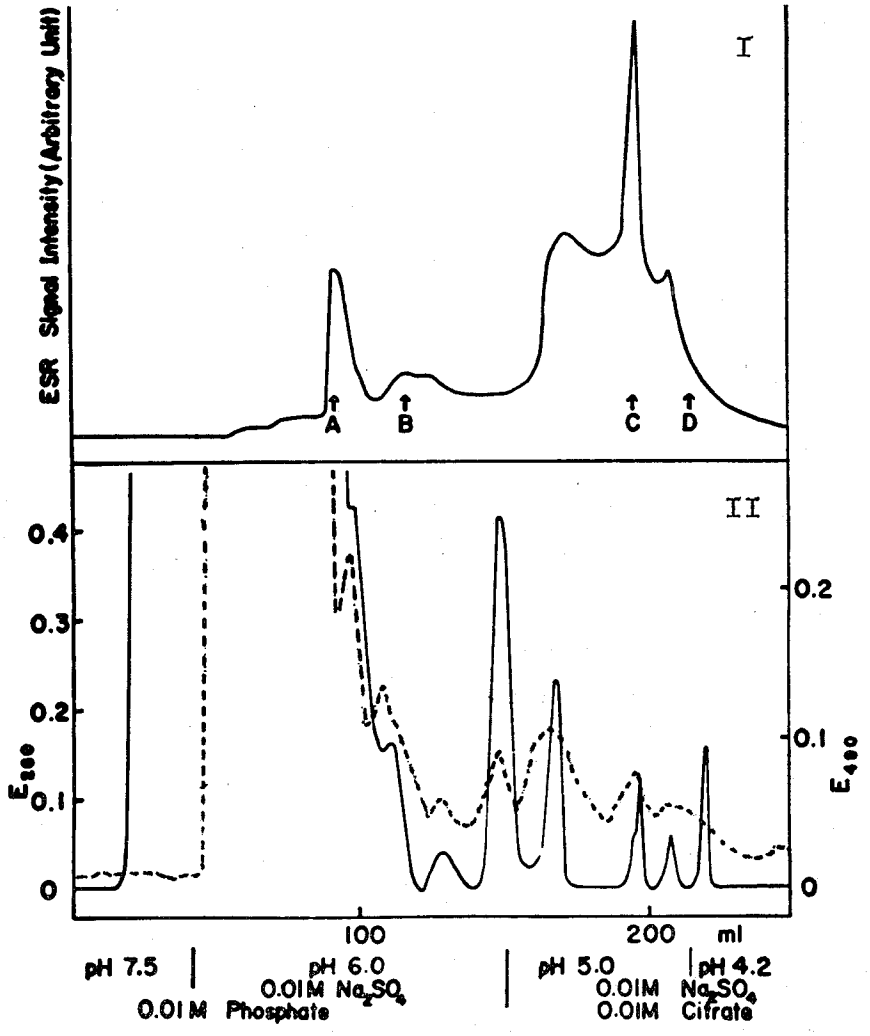

Fig. 3. Chromatogram of Spin Adducts of 5′-Thymidine monophosphate and 2-Methyl-2-nitrosopropane.
Experimental conditions: See Fig. 2; (I) ESR detection, (II) Orcinol-HCl detection ----, and UV detection ——

Four peaks appeared at the esr detection in Figs. 2, 3, and 4. The peak heights on the chromatograms are not really proportional to the radical concentration, because the esr intensity at the position of the fixed magnetic field is quite dependent on the line shapes of the esr spectra. The large peaks appeared at sugar and UV detections in the range of about 10 ml to 100 ml of the elution volume, which were due to the undamaged molecule in Figs. 2, 3, and 4. Typical esr spectra are shown in Figs. 8, 9, and 10. Abbreviations (A), (B), (C), and (D) correspond to the esr spectra measured for the fraction of A, B, C, and D in Figs. 2, 3, and 4 respectively.

Their esr parameters and other characteristics are listed in Table I. A sharp triplet has been found in the irradiated 5′-UMP solution and is attributed to di-t-butyl

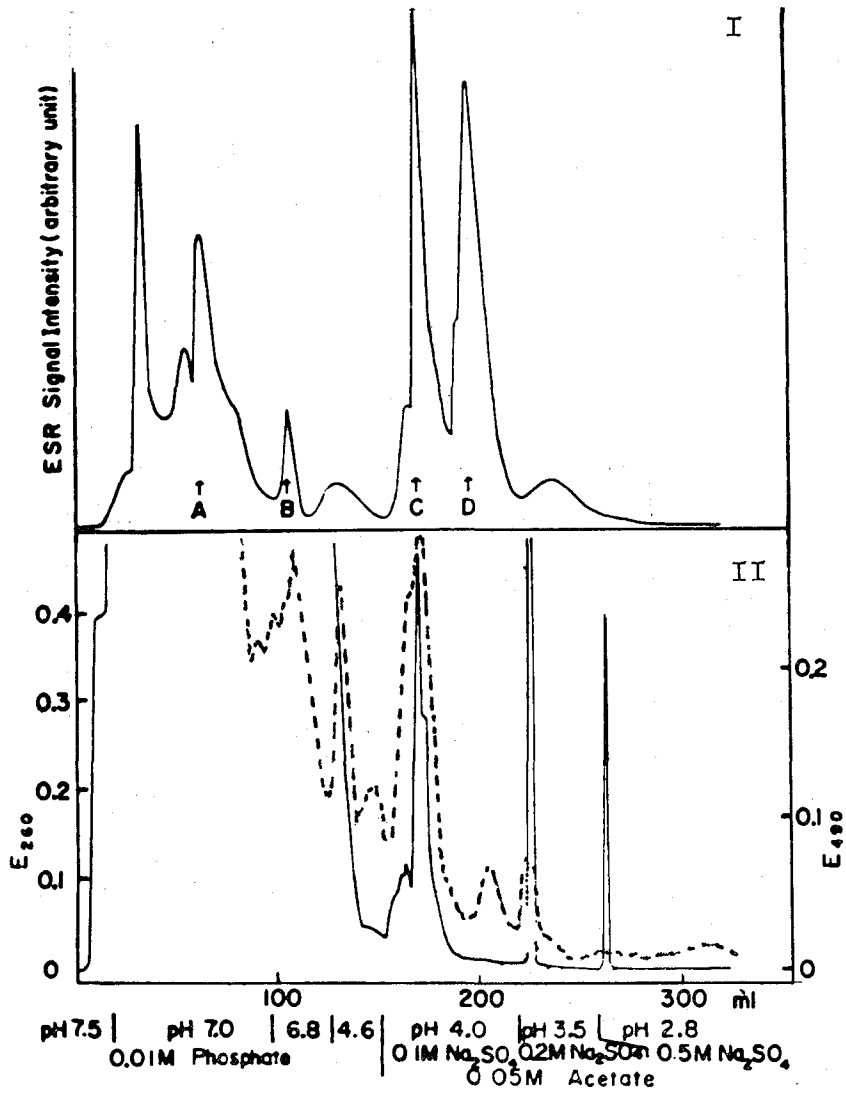

Fig. 4. Chromatogram of Spin Adducts of 5′-Cytidine monophosphate and 2-Methyl-2-nitrosopropane.
Experimental condition and explanation: See Fig. 3.

nitroxide radical, which is presented in Fig. 8(A). Figure 8(B) shows the esr spectrum for the fraction at the top of peak B, which was analysed as three groups of three lines with almost equal intensities and equal separation. The separation of the three groups was 14.3 G, which was due to hyperfine splitting of nitrogen nucleus of the NO group. The concentration of sugar almost reached a minimum at the fraction in peak B. Peak C had a sharp peak and a shoulder in the esr detection and corresponding sharp peaks were found by UV and by the orcinol method in the chromatogram in Fig. 2. The difference of the absorbances at 675 nm before and after reduction was less than 10 % of the maximum at this sharp peak, which indicated that 5,6-double

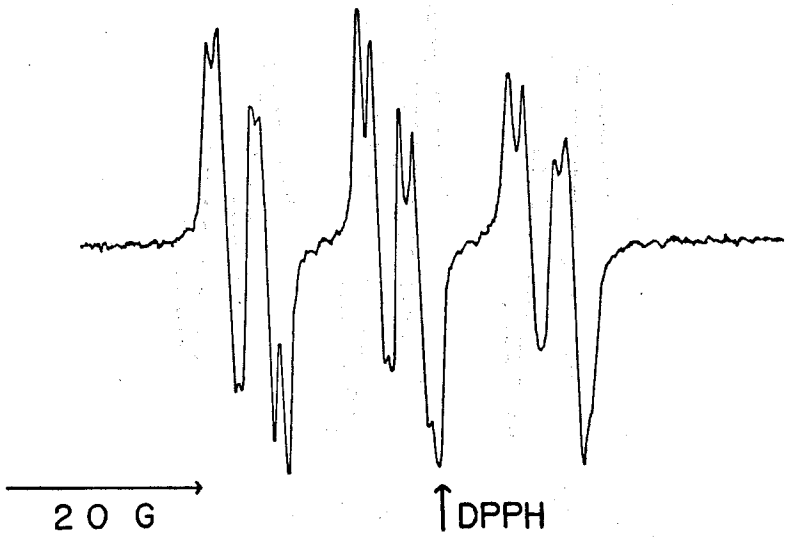

Fig. 5. ESR Spectrum of 5′-UMP Aqueous Solution Containing t-BuNO γ-Irradiated to 1.3×10^5 rads at ice temperature, and measured at room temperature immediately after the irradiation.

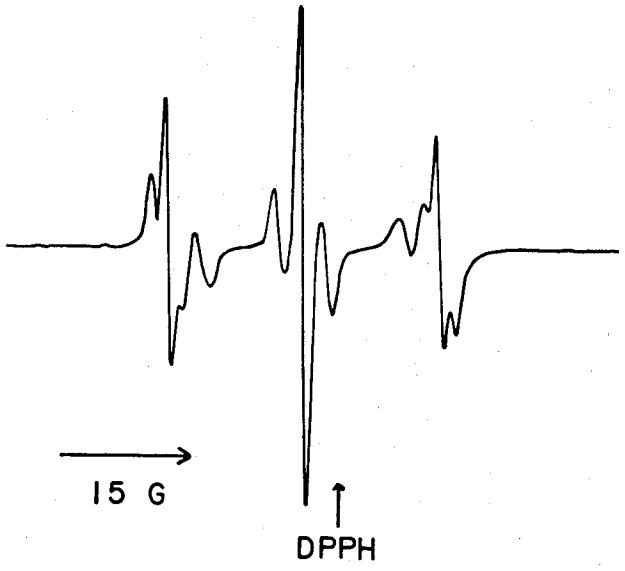

Fig. 6. ESR Spectrum of 5′-TMP Aqueous Solution Containing t-BuNO Experimental Conditions: See text and Fig. 5.

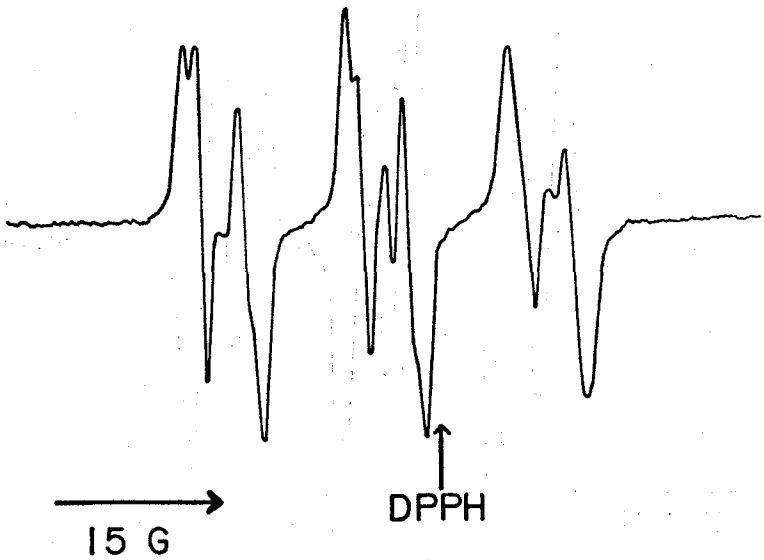

Fig. 7. ESR Spectrum of 5′-CMP Aqueous Solution Containing t-BuNO.
Experimental conditions: Same as in Figs. 5 and 6.

Table I. The Characteristics of the Trapped Radicals

Peak	a_N G	a_N and a_H G	Sugar	UV
		5′-Uridine monophosphate		
(A)	16.8			
(B)	14.3	a_N=3.0, triplet	−	
(C)	14.9	a_H=4.8, a_H=1.6, double-doublet	+	+
(D)	15.2	a_H=4.5, a_H=2.6, double-doublet	+	
		a_H=4.5, a_N=1.3, double-triplet		
		5′-Thymidine monophosphate		
(A)	14.9	a_H=4.9, doublet	+	
(B)	14.5	a_N=3.2, triplet		+
(C)	15.9		+	+
(D)	14.9	a_N=2.7, triplet	+	+
		5′-Cytidine monophosphate		
(A)	14.8	a_H=4.4, doublet		
(B)	15.2	a_H=5.4, doublet	+	
(C)	14.8	a_H=4.4, a_H=1.7, double-doublet	+	+
(D)	15.0	a_H=4.4, a_H=2.6, double-doublet	+	−
		a_H=4.4, a_N=1.3, double-triplet		

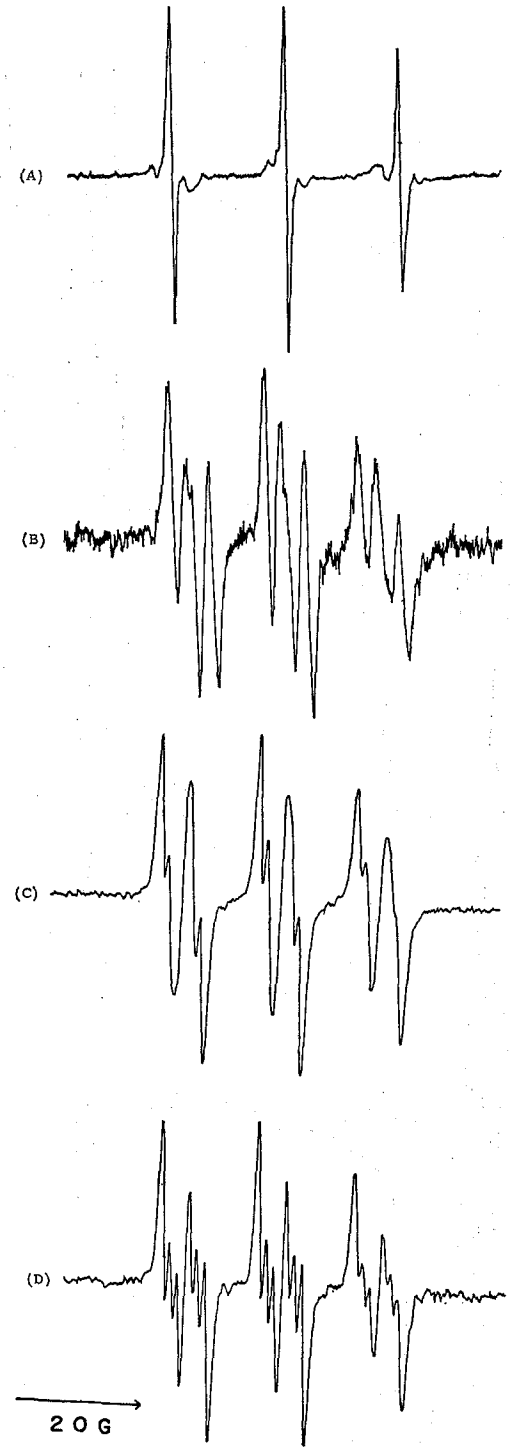

Fig. 8. ESR Spectra of Trapped Radicals of 5′-UMP γ-Irradiated after Separation by Liquid Chromatography.
(A), (B), (C), and (D) are ESR spectra for the peak A, B, C, and D respectively

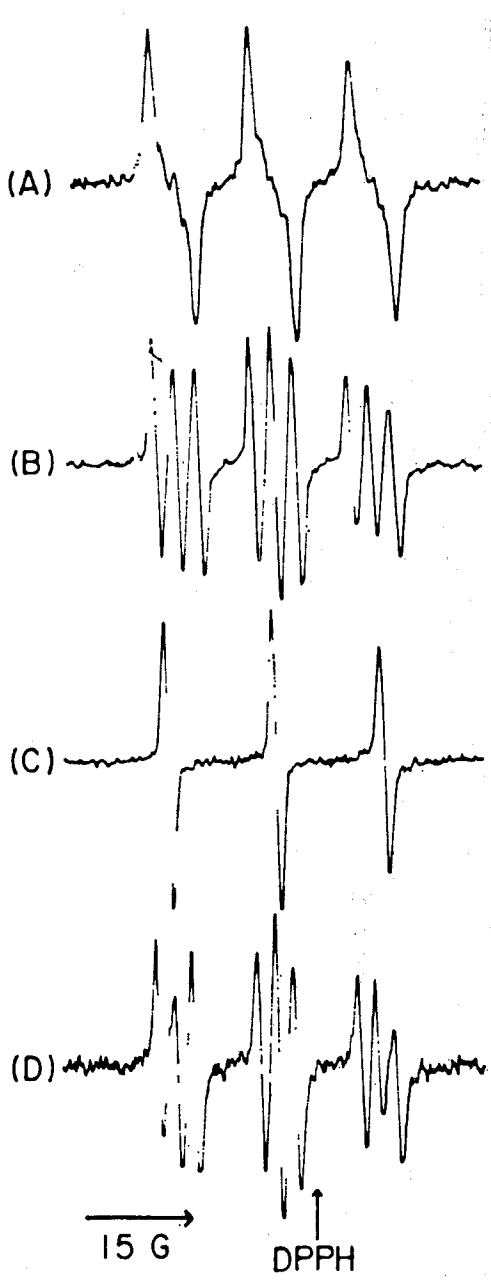

Fig. 9. ESR Spectra of Trapped Radicals of 5′-TMP γ-Irradiated after Separation by Liquid Chromatography.
(A), (B), (C), and (D) are ESR spectra for the peak A, B, C, and D respectively.

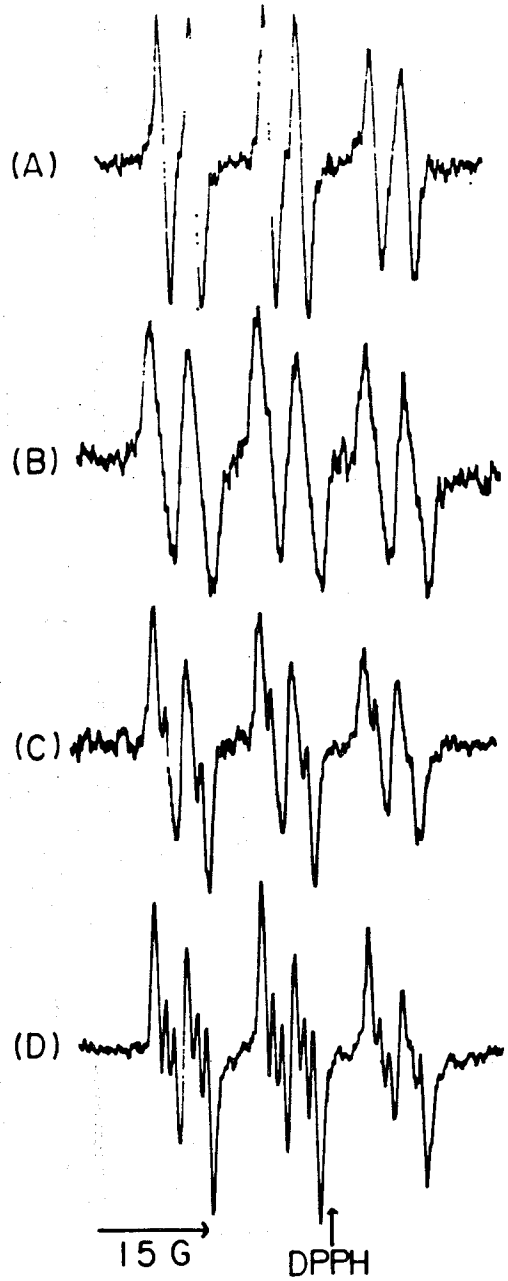

Fig. 10. ESR Spectra of Trapped Radicals of 5′-UMP γ-Irradiated after Separation by Liquid Chromatography.
(A), (B), (C), and (D) are ESR spectra for the peak A, B, C, and D respectively.

bond of the base might have already disappeared in the molecules eluted at this peak. There was a significant difference before and after reduction in absorbance at 675 nm at this shoulder and the radical species which were undamaged on the 5,6-double bond were eluted in this region. In the peak D in this figure, two peaks are superimposed and at the position of the sharp one, corresponding sharp UV and sugar peaks are found. The orcinol method showed no significant difference. At the broad peak, UV absorption was not detected, and the difference in absorbance at 675 nm was clearly found. It was concluded that the radical species in these two peaks were different. The sharp peak spectrum in Fig. 8(D) was analysed as three double-doublets and three double-triplets. The esr parameters obtained for these spectra are given in the table.

The esr spectrum of Fig. 9 (A) was analysed as three doublets superposed on some other signal, and that of Fig. 9 (B) was three groups of triplet with almost equal separation and equal intensities. The esr spectrum at the fraction of peak C was sharp triplet and corresponding peaks were found by the sugar and UV detections. Quite similar esr spectra were observed at the fractions in the left-side shoulder of peak C. The triplet-triplet in Fig. 9 (D) was observed at the right wing of the peak C, and in the fraction at the top of the right-side shoulder of the peak C. The esr spectrum was superposition of the signals of Fig. 9 (C) on those of Fig. 9 (D), where the contribution of the sharp triplet was quite large.

The esr spectra of Fig. 10 (A) and (B) were triplet-doublets and their splittings were a little different. There was a peak in the fraction of (B) in the sugar detection. The esr spectrum for the fraction in the peak at the left side of peak A was a superposition of the signal of di-t-butyl nitroxide radicals on the spectrum of Fig. 10 (A). At the position of peak C, corresponding peaks were found by UV and sugar detections and the double-doublet esr signal was observed in Fig. 10 (C). At the fraction of D there was a peak in sugar detection and no absorption was found by UV. The esr spectrum in Fig. 10 (D) was quite similar to that of Fig. 8 (D). The esr spectrum has been analysed as superposition of three groups of double-doublet on three double-triplets, based on the different contribution of those signals at different fraction. The same phenomenon was observed and the contribution of double-doublets was found more at right wing than at peak D.

The aerated aqueous solutions of constituents, uracil, uridine, and D-ribose, which constitute 5′-UMP, were γ-irradiated with t-BuNO. The esr spectrum of the uracil solution was similar to that reported for the same system[1,2] and the γ-irradiated uridine solution showed a similar esr spectrum to that of 5′-UMP. The trapped radicals in the D-ribose solution were very unstable and were only detected for the solution irradiated at ice temperature. The esr spectrum of the D-ribose solution irradiated to a total dose of 1×10^5 rad at ice temperature is shown in Fig. 11. Two superimposed species were analysed as that one was the same with in Fig. 8 and the other was a radical of three doublets with 1.8 G splitting. These doublets were apart by 14.9 G, and a centre of the signals was at the position of g=2.0058.

From these results, proposed radiolytic mechanisms to produce these radicals are summerized as follows:

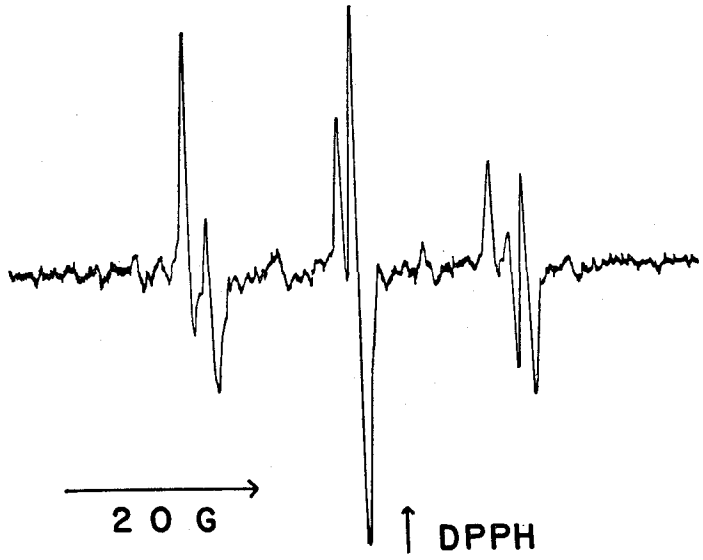

Fig. 11. ESR Spectra of a Trapped Radical of Ribose Fragment of 5′-TMP γ-Irradiated.

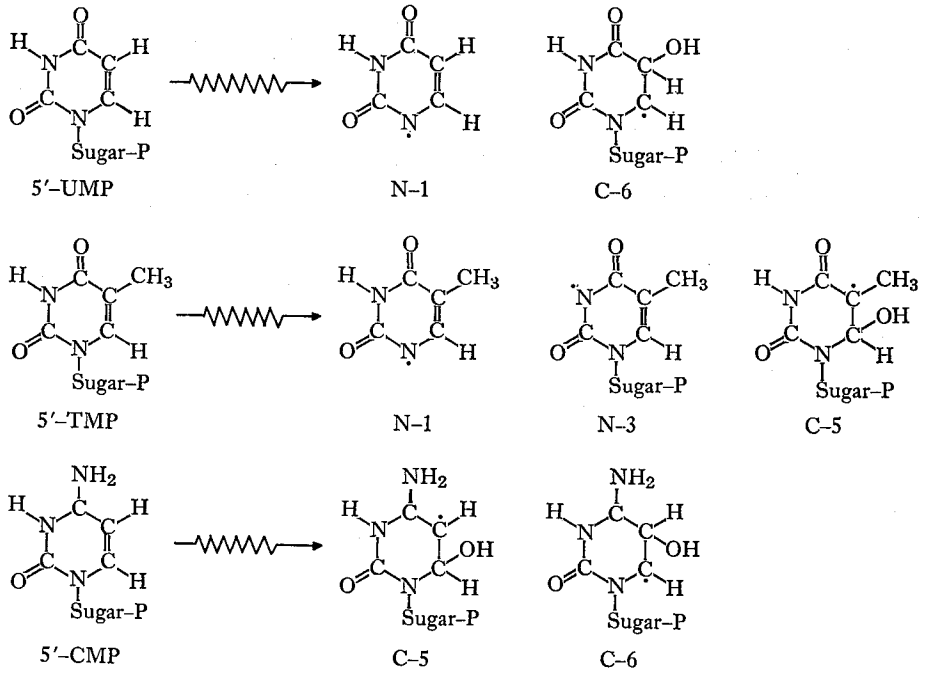

IV. DISCUSSION

1. Trapped Radicals in 5′-UMP

The radical which showed three lines in Fig. 8 (A) had a splitting of 16.8 G and g value of 2.0055. This radical is most probably di-t-butyl nitroxide which was reported to show $a_N=16.75$ G and $g=2.00556$ by Kawamura *et al.*[7] and to be observed by Perkins *et al.*[8,9] It was quite reasonable that no sugar was detected. No significant peak was detected by the orcinol method around peak B, and this meant that the N-C bond connecting the base and sugar was broken in the molecules eluted in peak B. It is probable that bond breakage makes a N-1 radical on the base, and the radical may be trapped by t-BuNO. The results of both of the orcinol and esr experiments show that the radical in peak B is the trapped N-1 radical (I). No N-3 radical has been reported on the γ-irradiated uracil or its derivatives. The esr spectrum of three double-doublets at the sharp part of peak C is attributed to a radical in which an unpaired electron on the NO group is interacting with two non-equivalent protons. The 5, 6-double bond of the base was broken at this radical, which was shown by the orcinol method, and it was probable that the radical at 5 or 6 position of the base was trapped by t-BuNO. The addition of an OH radical to the 5, 6-double bond of the base has been often reported as mentioned in the introduction. Two possible radical structures were assumed:

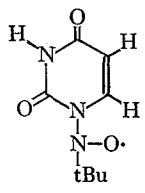

(I)

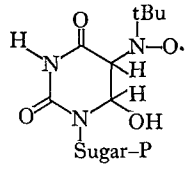

(II)

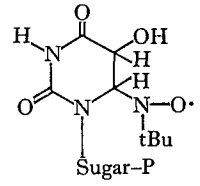

(III)

Two NO radical species were presumed at peak D, which showed the esr spectra of three double-doublets and three double-triplets. The radical structure (III) has one β-proton, one β-nitrogen, and one γ-proton, which is expected to show three double-triplets under the assumption that γ-proton cannot make any resolved splitting. The observed coupling constants of $a_H=4.5$ G and $a_N=1.3$ G are reasonable for the radical structure of (III)

The trapped radicals in this work were mainly base radicals. This does not mean that other parts of 5′-UMP are not damaged during γ-radiolysis.

2. Trapped Radicals in 5′-TMP

In this chromatography system with anion exchange resins, the molecules which had lost phosphate groups had to be eluted slower than those with phosphate group. It is difficult to find out plausible radical structure for Fig. 9 (A) and it might be due to the trapped molecular fragment of 5′-TMP. The esr spectra in Fig. 9 (B) and (D) are similar and these are attributed to radicals which have one nitrogen atom near by the NO groups. The possible radical structures are;

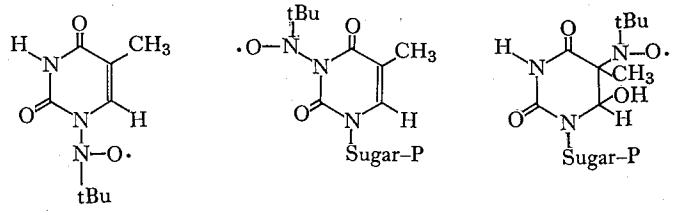

(IV) (V) (VI)

The radical of (V) has phosphate and sugar groups and is probably eluted later than radical (IV). In this context, the radical of Fig. 9 (B) is attributable to radical (IV) and that of Fig. 9 (D) is due to radical (V). This identification fits the results that no peak was observed by sugar detection around position of (B).

The esr spectrum of Fig. 9 (C) was sharp triplet and the unpaired electron of the trapped radical was not interacting well with hydrogen or nitrogen atom. The tradical of (VI) has four γ-protons around the NO group. Gamma-proton in the trapped radicals usually shows unresolved splitting. The structure (VI) was produced by addition of OH to the 5, 6-double bond of the base.

3. Trapped Radicals in 5′-CMP

Trapped radicals for Fig. 10 (A) and (B) showed three doublets. The unpaired electron in these radicals is interacting with one β-proton. Such a radical structure is possible at sugar residue, but the trapped sugar radical has been found to be very unstable at room temperature. The attack of OH to the 5,6-double bond makes two trapped radicals:

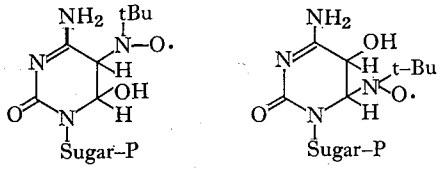

(VII) (VIII)

The radical (VII) could be attributed to the radical for Fig. 10 (B) rather than that for Fig. 10 (A). The suitable radical structure for Fig. 10 (A) cannot be assumed at this stage. The radical for Fig. 10 (C) have two non-equivalent β-protons around the NO group and have sugar residue in the molecule. The absorption of UV shows that the π-system of the base is not totally broken. The unstable sugar tradical is difficult to be assumed for this trapped radical. There are no position in the base where the trapped radicals could have two β-protons. This radical could not be identified by the simple consideration as the addition of OH or the abstruction of H by OH radicals. Two NO radical species were presumed for Fig. 10 (D), which showed the esr spectra of three double-doublets and three double-triplets. More contribution of double-doublets was found in the right wing of peak (D). The radical for double-triplets could be assumed to have one β-proton and one β-nitrogen around

the NO group. The radical structure of (VIII) fits this condition and the observed splitting of $a_H=4.4$ G and $a_N=1.3$ G are reasonable values for the structure (VIII). It is not easy to attribute the double-doublets to some radical structure in same sense of the identification of the radical for Fig. 10 (C).

ACKNOWLEDGMENT

The authors would like to express their thanks for using the facility of ^{60}Co-γ ray irradiation of The Institute for Chemical Research, Kyoto University

REFERENCES

(1) H. Taniguchi and H. Hatano, *Chem. Letters*, 531, (1975).
(2) H. Taniguchi and H. Hatano, *Chem. Letters*, 9, (1975).
(3) H. Taniguchi, S. Rokushika, and H. Hatano, *Anal. Letters*, **8**, 205 (1975).
(4) S. Kominami, S. Rokushika, and H. Hatano, *Int. J. Radiat. Biol.*, **30**, 525 (1976).
(5) S. Kominami, S. Rokushika, and H. Hatano, *Rad. Res.*, in press (1976).
(6) J. C. Stowell, *J. Org. Chem.*, **36**, 3055 (1971).
(7) T. Kawamura, S. Matsunami, and T. Yonezawa, *Bull. Chem. Soc. Japan*, **40**, 1111 (1967).
(8) M. J. Perkins and P. Ward, *J. Chem. Soc.*, (**B**) 395 (1970).
(9) M. J. Perkins and B. P. Roberts, *J. Chem. Soc.*, Perkin II, 173 (1974).